Determination of Total Widths and Resonance Energies of the Single-Particle Analog Resonances in ^{209}Bi*

W. R. WHARTON,† P. VON BRENTANO,‡ W. K. DAWSON,§ AND PATRICK RICHARD
Department of Physics, University of Washington, Seattle, Washington 98105
(Received 5 August 1968)

Excitation functions for the inelastic scattering of protons from ^{208}Pb have been obtained for incident proton energies from 14 to 18 MeV. Resonances corresponding to the first seven single-neutron isobaric analog states (IAR) of ^{209}Pb are observed. Many of the inelastic-scattering excitation functions show a resonance at only one of the IAR. These excitation functions were fitted with a five-parameter formula which consists of a resonance amplitude and an energy-independent background amplitude. For some excitation functions, additional resonance amplitudes were included. The analogs of the $g_{9/2}$ (ground-state), $i_{11/2}$(0.79-MeV), $j_{15/2}$ (1.41-MeV), $d_{5/2}$ (1.56-MeV), $s_{1/2}$ (2.03-MeV), $g_{7/2}$ (2.47-MeV), and $d_{3/2}$ (2.52-MeV) states are found to have total widths of 253±10, 224±20, 201±25, 308±8, 319±15, 288±20, and 279±20 keV, respectively. In respective order, the resonance laboratory energies are 14.918±0.006, 15.716±0.010, 16.336 ±0.015, 16.496±0.008, 16.965±0.014, 17.430±0.010, and 17.476±0.010 MeV.

I. INTRODUCTION

THE single-neutron isobaric analog resonances (IAR) observed in proton elastic and inelastic scattering from ^{208}Pb have been studied by several groups,[1–4] and the total widths Γ, resonance energies E_R, and the elastic proton partial widths Γ_{P_0} have been obtained from the elastic scattering excitation function. Since all the single-particle states are present in the elastic scattering channel, the extraction of the resonance parameters from the elastic scattering is subject to the following difficulties: (a) The total widths are relatively large compared to the level spacings; (b) each resonance shows a large interference pattern because of the large background cross section; and (c) one of the most sensitive parameters in fitting the data is Γ_{P_0}/Γ and not Γ_{P_0}, since the former quantity determines the magnitude of the interference effect on resonance. Therefore, Γ_{P_0} is determined only as well as Γ is determined.

In contrast to the above properties of the elastic scattering, the inelastic scattering excites strongly and selectively various bands of states in the final ^{208}Pb nucleus.[4,5] In other words, many of the inelastic channels resonate at only one or possibly two of the single-particle states. In addition, the off-resonance cross section to these states is often very small compared to the resonance cross section, thus minimizing the effects of interference.

The structure of the inelastic scattering can be made quantitative in the shell-model description of the states in ^{209}Pb and ^{208}Pb. The final excited states Ψ_I of ^{208}Pb can be decomposed into neutron particle-hole configurations and proton and collective configurations $\Psi_I{}^P$ so that

$$\Psi_I=\sum_{Jj}(j^{-1}J)_I a_{IjJ}+\Psi_I{}^P. \quad (1)$$

In this expression the parentheses stand for vector coupling and a_{IjJ} is a parentage coefficient. The single-neutron state in ^{209}Pb of spin J, isospin T is

$$\Psi(J,T,T)=\nu(J)\phi_c(0^+), \quad (2)$$

and the analog of this state in ^{209}Bi is

$$\Psi^{\mathrm{IAR}}(J,T,T-1)$$
$$=[T_-/(2T)^{1/2}]\Psi(J,T,T)$$
$$=(2T)^{-1/2}[\pi(J)\phi_c(0^+)+\nu(J)T^-\phi_c(0^+)], \quad (3)$$
$$T^-\phi_c(0)^+=\sum_j(2j+1)^{1/2}[(\pi(j)\nu^{-1}(j))0^+]\phi_c(0^+), \quad (4)$$

where ϕ_c is the ground state of ^{208}Pb, $\nu(j)$ [or $\pi(j)$] is the wave function for the neutron (or proton) in the j orbit. Elastic scattering occurs via the nonzero overlap of the target ground state with the first term in Eq. (3), whereas inelastic scattering occurs via the overlap of the target excited state with the last terms in Eq. (3), which can be rewritten as

$$\frac{1}{(2T)^{1/2}}\nu(J)\phi_c(0^+)\sum_j(2j+1)^{1/2}[(\pi(j)\nu^{-1}(j))0^+]$$
$$=\frac{1}{(2T)^{1/2}}\sum_j(2j+1)^{1/2}|(J(j^{-1}j)0^+)J\rangle. \quad (5)$$

The overlap for inelastic scattering to a final state Ψ_I

* Work supported in part by the U. S. Atomic Energy Commission.
† Present address: Center for Nuclear Studies, Austin, Texas 78712.
‡ On leave from Max Planck Institut für Kernphysik, Heidelberg, Germany.
§ Visiting Professor on leave from Nuclear Research Center, University of Alberta, Edmonton, Alberta, Canada.
[1] C. D. Kavaloski, J. S. Lilley, P. Richard, and N. Stein, Phys. Rev. Letters **16**, 807 (1966).
[2] G. H. Lenz and G. M. Temmer, Phys. Letters **24B**, 370 (1967); Nucl. Phys. **A112**, 625 (1968).
[3] S. A. A. Zaidi, J. L. Parish, J. G. Kulleck, C. Fred Moore, and P. von Brentano, Phys. Rev. **165**, 1312 (1968).
[4] N. Stein and D. A. Bromley, Phys. Rev. Letters **20**, 113 (1968).
[5] C. F. Moore, J. G. Kulleck, P. von Brentano, and F. Rickey, Phys. Rev. **164**, 1559 (1967).

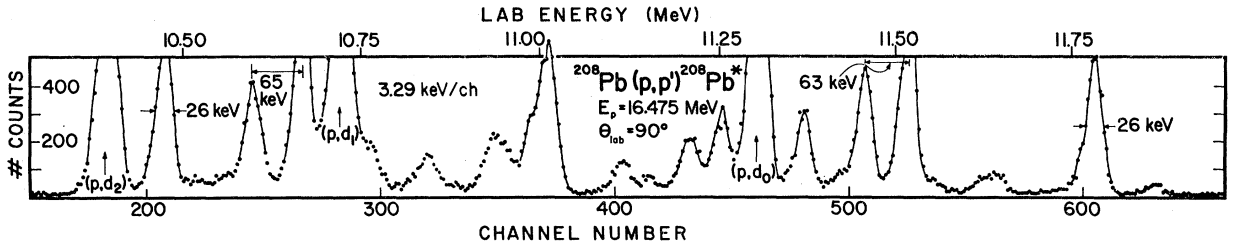

FIG. 1. Spectrum of the reaction ^{208}Pb$(p,p')^{208}$Pb* at $E_p^{\text{lab}}=16.475$ MeV and $\theta_{\text{lab}}=90°$. FWHM of 26 keV is indicated for two of the peaks.

leads to an observed width[6] $\Gamma_{P'}=\sum_j \Gamma_{IjJ}{}^{P'}$, where

$$\Gamma_{IjJ}{}^{P'}=\left(\frac{2I+1}{2J+1}\right)\Gamma_j{}^{SP}|a_{IjJ}|^2. \tag{6}$$

By observing which single-neutron states J are excited in each inelastic channel, the particles in the particle-hole configurations are determined. In most cases, however, the spin of the state I and the neutron holes j for which $a_{IjJ}\neq 0$ are still unknown. The latter information can in principle be determined or partly determined from a study of the angular distribution of each inelastic group at energies on and off the resonance.[6,7] A fourthcoming publication will treat this problem more fully.[8]

In summary, from the inelastic scattering excitation functions we determine (a) the particles J forming the neutron contribution to the neutron particle-hole configurations of the state Ψ_I, (b) the total resonance widths, (c) the resonance energies, and (d) the ratio of the on-resonance to off-resonance cross sections, which is important for doing further investigation of angular distributions.

II. EXPERIMENTAL PROCEDURE

Proton beams of $\sim$0.5 μA were obtained from the University of Washington three-stage FN tandem Van de Graaff for the energy range 14–18 MeV. The beam was energy analyzed by a 90° magnet and was further magnetically deflected by a switching magnet into a 60-in. scattering chamber. The energy analysis system is calibrated to $\pm$10 keV [9] in the energy range of interest and the resultant beam has a nominal energy spread of $\leq$1 keV as measured by the Van de Graaff terminal ripple.

The targets used in the experiment were made from 99% enriched ^{208}Pb. The metal was evaporated onto glass slides, floated off onto deionized water in an argon atmosphere, and subsequently lifted onto $\frac{1}{2}$-in.-diam aluminum inserts. The targets, when not in use, were placed in a sealed dessicator filled with argon and placed in a freezer in order to prevent oxidation. Care was taken in removing the targets from the frigid environment so as to prevent condensation from forming on the targets.

In order to obtain an accurate excitation function, two major problems must be kept in mind. (a) The levels of ^{208}Pb are very closely spaced so that a very good energy resolution is necessary. (b) The inelastic scattering cross sections are relatively small (from a few to a few hundred μb) and the peaks fall in energy below the elastic peak making it necessary to reduce slit-edge scattering effects. With these points in mind we set out to obtain $\sim$26-keV resolution for 12-MeV protons in a solid-state detector thick enough to stop the full energy protons ($\sim$18 MeV). The final system consisted of carefully selected Si(Li) detectors that were made in the laboratory.[10] We normally ran with two detectors simultaneously, which were cooled in the chamber by thermoelectric coolers. Gold foils $\sim$300 μg/cm^2 were placed in front of the detectors in order to eliminate electrons eminating from the target and to subsequently improve the resolution and peak shapes. Magnets were also placed in front of each detector for the purpose of removing electrons. Tennelec TC130 preamplifiers[11] were used followed by ORTEC 220 amplifier-biased amplifier systems.[12] Pulses corresponding to particles in the energy range 8–12 MeV were fed into analog-to-digital converters and stored as 1024-channel spectra by the on-line SDS 930 computer.

Figure 1 contains a typical spectrum obtained with this sytem. The resolution is 26 keV; however, for part of the data the resolution obtained was approximately 32 keV. The ratio of elastic peak to background was as high as 20 000 to 1, which gave an inelastic-peak-to-background ratio as large as 300 to 1 for some peaks.

III. ANALYSIS PROCEDURE

The inelastic scattering excitation functions may be described by a collision matrix consisting of a background term and one or more Breit-Wigner resonance

[6] P. Richard, W. G. Weitkamp, W. Wharton, H. Wieman, and P. von Brentano, Phys. Letters **26B**, 8 (1967).
[7] J. Bondorf, P. von Brentano, and P. Richard, Phys. Letters **27B**, 5 (1968).
[8] P. Richard, H. Wieman, W. Wharton, P. von Brentano, and W. Weitkamp (unpublished).
[9] N. Mangelson and J. G. Cramer (private communication).
[10] University of Washington 1968 Progress Report, p. 158 (unpublished).
[11] Tennelec Corp., Oak Ridge, Tenn.
[12] ORTEC, Inc., Oak Ridge, Tenn.

terms.[13,14] In particular, a collision matrix with one resonance term will lead to a cross section of the form

$$\sigma(\theta,E)=\sum_\beta\left|A_\beta(\theta)+\frac{iB_\beta(\theta)e^{i\alpha_\beta(\theta)}}{(E-E_0)+i\frac{1}{2}\Gamma}\right|^2. \quad (7)$$

Here all the parameters are real and we have assumed A_β, B_β, and α_β are energy-independent. The sum is taken over the spin channels $\beta=(M_T,M_P,M_T',M_P')$ of the reaction. From Eq. (7) we immediately obtain a fit formula for the cross section

$$\sigma(\theta,E)=\sigma_D+\frac{\sigma_0\frac{1}{4}\Gamma^2+\frac{1}{2}(E-E_0)S\Gamma}{(E-E_0)^2+\frac{1}{4}\Gamma^2}, \quad (8)$$

where we have

$$\sigma_D=\sum_\beta|A_\beta|^2=\sigma(\theta,\infty),$$
$$\sigma_0=\sum_\beta(B_\beta^2+A_\beta B_\beta\Gamma\cos\alpha_\beta)=\sigma(\theta,E_0)-\sigma_D, \quad (9)$$
$$S=\sum_\beta\frac{-4A_\beta B_\beta}{\Gamma}\sin\alpha_\beta=\sigma(\theta,E_0+\tfrac{1}{2}\Gamma)-\sigma(\theta,E_0-\tfrac{1}{2}\Gamma).$$

It is important to note that σ_0 is not the pure resonance amplitude but contains interference terms. In fact, the angular distribution at $E-E_0$ is different from that of an isolated resonance because of the interference terms in σ_0, since the S term does not contribute at $E=E_0$. The two-level formula is a simple extension of Eq. (8), namely,

$$\sigma(\theta,E)=\sigma_D+\frac{\frac{1}{4}\sigma_0\Gamma^2+\frac{1}{2}(E-E_0)S\Gamma}{(E-E_0)^2+\frac{1}{4}\Gamma^2}+\frac{\frac{1}{4}\sigma_0'\Gamma'^2+\frac{1}{2}(E-E_0')S'\Gamma'}{(E-E_0')^2+\frac{1}{4}\Gamma'^2}. \quad (10)$$

σ_0 and S (σ_0' and S') in Eq. (10) include additional terms representing interference between the two resonances and they can no longer be defined by Eq. (9).

The procedure for analyzing the data may be divided into several steps.

(a) A least-squares fit using Eq. (8) was obtained for excitation functions showing one resonance. All five parameters were allowed to vary simultaneously and values of E_0 and Γ for six resonances (all except the $s_{1/2}$ resonance) were subsequently obtained.

(b) A least-squares fit using Eq. (10) was then obtained for excitation functions showing two resonances. Using the values from step 1 as initial parameters, Γ and E_0 for one of the two resonances were held fixed while Γ and E_0 for the other resonance was allowed to vary simultaneously with the remaining five parameters. Values of E_0 and Γ were subsequently obtained for the $s_{1/2}$ resonance and other resonances.

(c) The results of step 2 were combined with the results of step 1 to obtain new values for Γ and E_0 for all resonances. Step 2 was then repeated.

(d) A least-squares fit for excitation functions showing three resonances was obtained using a three-level fit formula. Γ and E_0 for two of the resonances were held fixed at values obtained in step 3. Γ and E_0 for the remaining resonance were allowed to vary simultaneously with the remaining seven parameters.

One of the major assumptions of the analysis as discussed in this section is that of an energy-independent background amplitude. As a test of the extent to which this introduces errors in the analysis we also analyzed the excitation function using an energy-dependent background amplitude

$$A_\beta\rightarrow A_\beta+A_\beta'(E-E_0),\quad A_\beta'/A_\beta\ll1. \quad (11)$$

Keeping only the first-order terms in A_β', we obtain

$$\sigma(\theta,E)=\sigma_D+(E-E_0)\sigma_1+\frac{\frac{1}{4}\sigma_0\Gamma^2+\frac{1}{2}(E-E_0)S\Gamma}{(E-E_0)^2+\frac{1}{4}\Gamma^2}. \quad (12)$$

The first-order approximation is valid in the energy region near E_0, the resonance energy.

IV. EXPERIMENTAL RESULTS AND ANALYSIS

A. Inelastic Scattering on ^{208}Pb

Inelastic proton scattering excitation functions for the ^{208}Pb(p,p') reaction were taken from 14.2 to 18.3

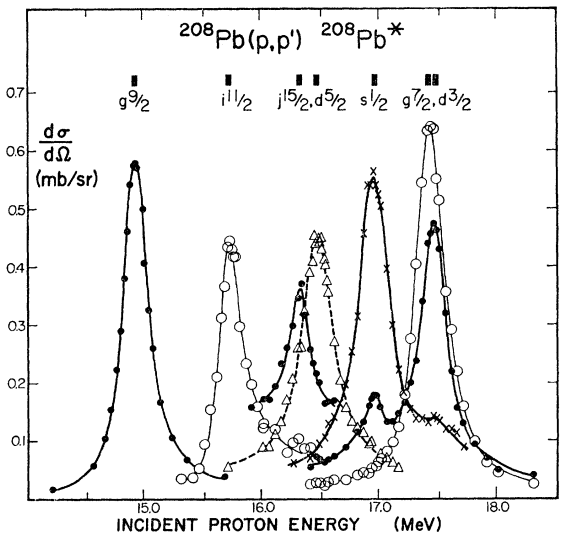

FIG. 2. Excitation functions near each IAR in ^{209}Bi* for selected final states in ^{208}Pb: 3.469-MeV state at 90° near $g_{9/2}$ resonance; 5.071-MeV state at 90° near $i_{11/2}$ resonance ($d\sigma/d\Omega\times3$); 4.602-MeV state at 158° near $j_{15/2}$ resonance ($d\sigma/d\Omega\times10$); 5.804-MeV state at 90° near $d_{5/2}$ resonance; 6.304-MeV state at 90° near $s_{1/2}$ resonance ($d\sigma/d\Omega\times3$); 5.958-MeV state at 100° near $g_{7/2}$ resonance; 5.915-MeV state at 100° near $d_{3/2}$ resonance ($d\sigma/d\Omega\times2$).

[13] H. A. Weidenmüller, Nucl. Phys. **A99**, 289 (1967).

[14] K. W. McVoy, in *Lectures on Fundamentals in Nuclear Theory*, edited by A. DeShalit and C. Villi (International Atomic Energy Agency, Vienna, 1967).

MeV incident proton energies in energy steps varying from 100 to 10 keV. The relative positions of the single-particle analog resonances are indicated in Fig. 2, which contains seven excitation functions to selected ^{208}Pb final states, each being excited predominantly at only one of the single-particle analog states in ^{209}Bi.* Further discussion of the inelastic scattering will be divided according to the ^{209}Bi single-particle analog resonances. Inelastic scattering excitation functions that contain two or more resonances will be discussed in each appropriate section. A table of results for each resonance summarizes the results of the analysis of all the inelastic scattering excitation functions. Also, a figure will be given for several experimental excitation curves with the best least-squares fit indicated by a solid curve. The resonances that were included in each fit are indicated in each figure by an arrow.

TABLE I. Parameters for $g_{9/2}$ resonance.

^{208}Pb state E_{ex} (MeV)	I^π	θ_{lab}	E_0 (MeV)	Γ (keV)	σ_D (mb/sr)	σ_0/σ_D	N[a]
3.192	5^-	89.9°	14.914	258	0.066	6.3	1
		149.3°	14.916	246	0.072	5.0	1
3.469	4^-	89.9°	14.920	255	0.010	56.6	1
		149.3°	14.934	250	0.012	30.0	1
3.702	5^-	89.9°	14.914	247	0.016	13.8	1
		149.3°	14.913	231	0.008	9.5	1
3.913		89.9°	14.909	242	0.005	29.2	1
3.992		89.9°	14.909	281	0.005	18.6	1
4.032		89.9°	14.922	234	0.003	47.7	1
4.174	(5^-)	89.9°	14.918	264	0.003	65.4	1
4.252		89.9°	14.925	297	0.006	28.5	1
4.289	(5^-)	89.9°	14.912	283	0.020	12.2	1
4.351	(4^-)	89.9°	14.915	256	0.009	29.3	1
4.475	(6^-)	89.9°	14.920	249	0.005	49.4	1
		149.3°	14.918	258	0.013	33.6	1
4.692	3^-	149.3°	14.924	241	~0.030[b]	3.8	3

[a] N is the number of resonances observed in that particular channel and included in the fit.
[b] See caption of Table IV, $\sigma_1 = 0.009$.

The excitation functions shown in the figures are often not extended over the region where they show at most very weak resonances. In some cases we combined the results at two angles (90° with 100° or 149.3° with 158°) in order to obtain a complete excitation function. A slight renormalization was generally made to match the excitation function at one angle with the excitation function at the other angle (see Figs. 4, 7, 8, 10, and 11).

1. $g_{9/2}$ Ground-State Resonance

Excitation functions for 12 final states in the proton inelastic scattering were recorded in the vicinity of the $g_{9/2}$ ground-state IAR. These 12 final states occur between 3.1- and 4.7-MeV excitation in ^{208}Pb. Figure 3 contains excitation functions for four of the final states which resonate mainly at the $g_{9/2}$ resonance. The remaining eight states analyzed have cross sections $\sigma_0 \leq 200$ μb/sr except for the 4.289- and 4.351-MeV states. These excitation functions have errors because of

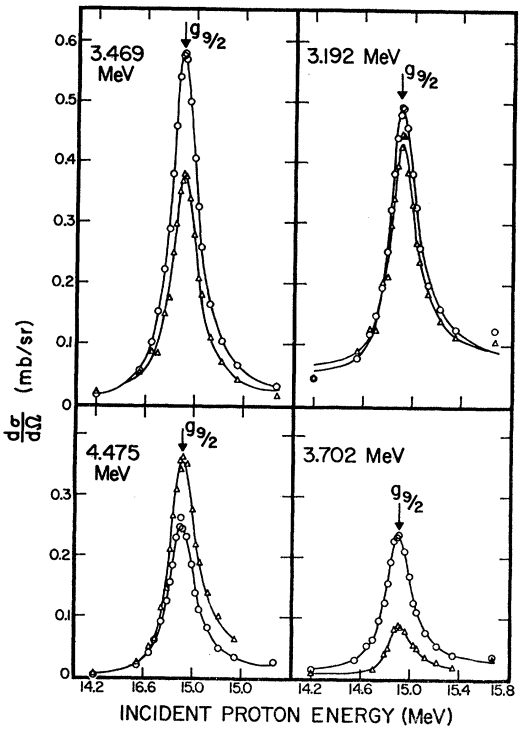

FIG. 3. ^{208}Pb $(p,p')^{208}$Pb* excitation functions near the $g_{9/2}$ IAR to the ^{208}Pb final states indicated. The open circles represent data taken at $\theta_{lab} = 89.9°$, and the open triangles represent data taken at $\theta_{lab} = 149.3°$. The arrows indicate which resonances were included in the least-squares fit, which is indicated by the solid curves. The error bars have been left off for convenience but are about twice the size of the circles (triangles) for most points.

the closely spaced levels. The 4.692-MeV state is observed to resonate at the $g_{9/2}$, $i_{11/2}$, and $d_{5/2}$ states[3] and was fit with a three-resonance formula (see Fig. 4).

These results of the least-squares fit to the data are summarized in Table I. The values of σ_D, σ_0/σ_D, E_0, and Γ as defined in Sec. II are given for each excitation function. The values of E_0 are consistent for all the fits and gives a weighted average value of 14.918±0.006

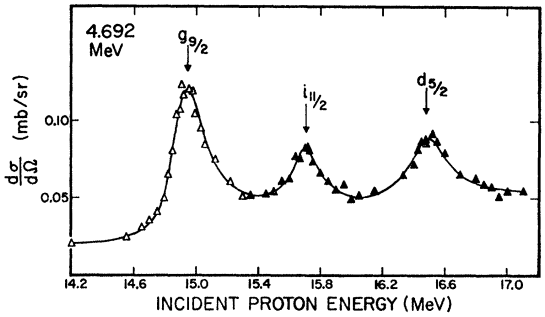

FIG. 4. ^{208}Pb$(p,p')^{208}$Pb (4.692-MeV) excitation curve at $\theta_{lab} = 149.3°$ below 15.35 MeV normalized to match the excitation curve for $\theta_{lab} = 158°$ above 15.35 MeV. The least-squares fit (solid curve) is made with an energy-dependent background (see text). Γ and E_0 are held fixed at the values given in Table VIII for each resonance.

TABLE II. Parameters for $i_{11/2}$ resonance.

^{208}Pb state E_{ex}(MeV)	θ_{lab}	E_0 (MeV)	Γ (keV)	σ_D (mb/sr)	σ_0/σ_D	N[a]
4.200	90.0°	15.731	212	0.009	8.7	1
4.692	158.0°	15.712	246	0.035[b]	2.2	3
4.928	158.0°	15.714	241	0.001	18.0	1
5.071	90.0°	15.710	235	0.013	10.0	1
	158.0°	15.710	215	0.007	13.7	1

[a] See caption of Table I.
[b] See caption of Table IV, $\sigma_1=0.009$.

MeV. The total width Γ determination shows a larger spread in values and has a weighted average of 253±15 keV. It is found that the error in Γ is much reduced by considering only those excitation functions for which $\sigma_0 \geq 250$ μb/sr, whereas the values of Γ, E_0, and ΔE_0 are unaffected. This subset of data yields $\Gamma=253\pm4$ keV and $E_0=14.919\pm0.006$ MeV.

2. $i_{11/2}$ (0.79-MeV) Analog Resonance

Near the resonance energy for the $i_{11/2}$ IAR the cross sections to four states were large enough to allow extraction of an excitation function. Table II contains a summary of the results and Fig. 5 contains experimental excitation functions and the fits to three of the final states. The excitation function for the fourth state (4.692 MeV) is given in Fig. 4.

The cross sections σ_0 are all ≤ 130 μb/sr and the values of σ_0/σ_D are not as large as for the $g_{9/2}$ resonance. The resonance parameters E_0 and Γ are, nonetheless, rather consistent and have weighted averages of 15.716±0.010 MeV and 224±15 keV.

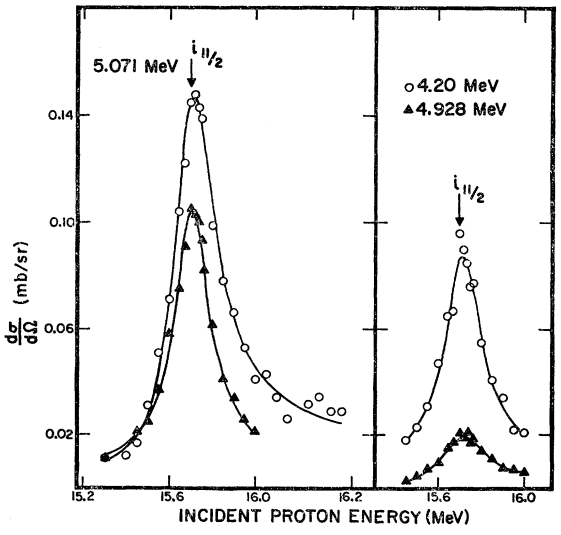

FIG. 5. ^{208}Pb$(p,p')^{208}$Pb* excitation functions near the $i_{11/2}$ IAR to the ^{208}Pb final states indicated. The open circles represent data taken at $\theta_{lab}=90°$, and the closed triangles represent data taken at $\theta_{lab}=158°$. See also caption of Fig. 3.

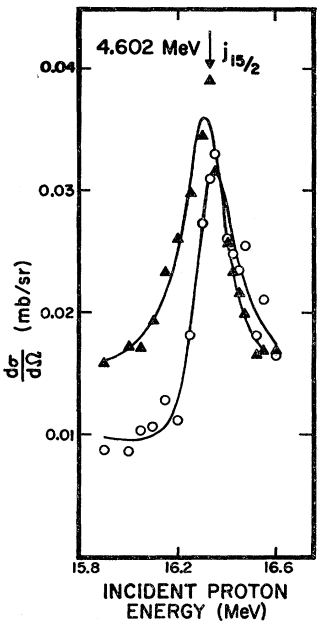

FIG. 6. ^{208}Pb$(p,p')^{208}$Pb (4.602) excitation functions near the $j_{15/2}$ IAR. See also caption of Fig. 5.

3. $j_{15/2}$ (1.42-MeV) Analog Resonance

The 4.602-MeV state in ^{208}Pb was observed to resonate at the $j_{15/2}$ resonance at both 90° and 158° (see Fig. 6). There is appreciable nonresonance cross section observed at both angles which causes the resonance shapes to be quite different from each other. The consistent determination of E_0 and Γ as given in Table III is encouraging and gives evidence that the form of the equations chosen for the analysis is correct. The errors quoted in this table are fitting errors alone and do not include systematic errors. The unresolved 4.835 and 4.857 states[5] were also seen to resonate at the $j_{15/2}$ but were not analyzed.

4. $d_{5/2}$ (1.56-MeV) Analog Resonance

More data points were taken near the $d_{5/2}$ resonance than near any other resonance. The accuracy of the work is reflected in the consistency of Γ and E_0 for the first three states in Table IV. The excitation functions for the last three states at 5.804, 5.869, and 6.000 MeV (see Fig. 7) each show two other resonances and extend over such a large energy range that we were probably unjustified in using energy-independent parameters. Therefore, we have included in Table IV the fits obtained using the background energy dependence

TABLE III. Parameters for $j_{15/2}$ resonance.

^{208}Pb state E_{ex}(MeV)	θ_{lab}	E_0 (MeV)	Γ (keV)	σ_D (mb/sr)	σ_0/σ_D
4.602	90.0°	16.333±0.013	194±22	0.012	1.5
	158.0°	16.338±0.010	208±23	0.014	1.6

TABLE IV. Parameters for $d_{5/2}$ resonance. For some states, an energy-dependent background term $(E-E_0)\sigma_1$ was added to the fit formula [see Eq. (12)] and new values for E_0 and Γ were obtained.

^{208}Pb state E_{ex}(MeV)	θ_{lab}	E_0 (MeV)	Γ (keV)	σ_D (mb/sr)	σ_1 (mb/sr MeV)	σ_0/σ_D	N[a]
4.967	90°	16.498	303	0.044	···	8.0	2
4.967	158°	16.490	316	0.035	···	3.4	2
5.030	90°	16.497	307	0.013	···	21.8	1
5.030	158°	16.493	308	0.005	···	28.0	1
5.121	90°	16.494	299	0.013	···	12.5	1
5.121	158°	16.507	307	0.003	···	23.1	1
5.804	90°–100°	16.491	319	0.031	···	13.5	3
5.804	90°–100°	16.497	322	···	0.007		
5.869	90°–100°	16.495	324	0.018	···	14.8	3
5.869	90°–100°	16.504	308	···	0.010		
5.869	158°	16.506	318	0.004	···	46.3	3
5.869	158°	16.511	312	···	0.002		
6.000	90°–100°	16.473	320	0.064	···	5.0	3
6.000	90°–100°	16.486	313	···	0.015		
6.000	158°	16.492	319	0.048	···	8.0	3
6.000	158°	16.496	314	···	0.002		

[a] See caption of Table I.

given in Eq. (12). The fits of the excitation functions for the state at 4.967 MeV indicate the presence of an $s_{1/2}$ resonance. At 158°, the fit using the one-level formula gave $\Gamma_{d_{5/2}}=334$ keV, $E_{d_{5/2}}=16.488$ MeV, and $\chi^2=7.2$. The fit using the two-level formula with the second resonance being the $s_{1/2}$ resonance gave $\Gamma_{d_{5/2}}=316$ keV, $E_{d_{5/2}}=16.490$ MeV, and $\chi^2=3.9$, where

$$\chi^2=\sum_{\text{all data}}\frac{(\sigma_{\text{fit}}-\sigma_{\text{expt}})^2}{(\sigma_{\text{expt error}})^2}.$$

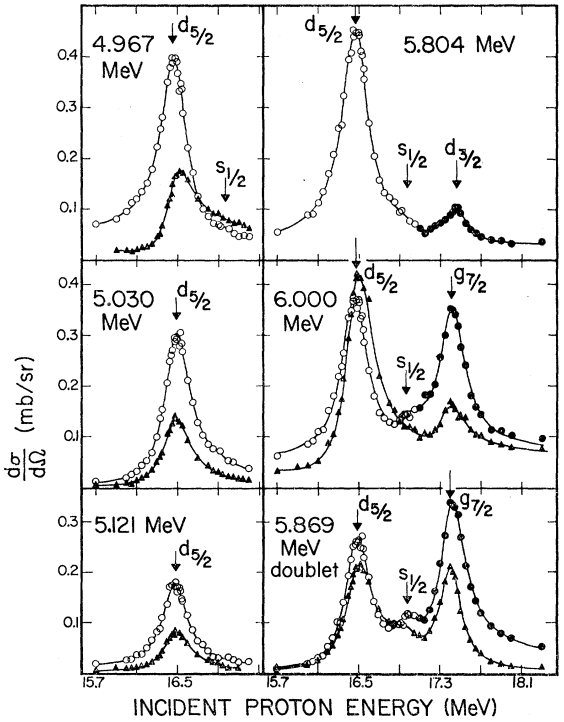

FIG. 7. ^{208}Pb$(p,p')^{208}$Pb excitation functions near the $d_{5/2}$ IAR. See also caption of Fig. 5. The closed circles are data at $\theta_{lab}=100°$ normalized to match the data at $\theta_{lab}=90°$ (open circles).

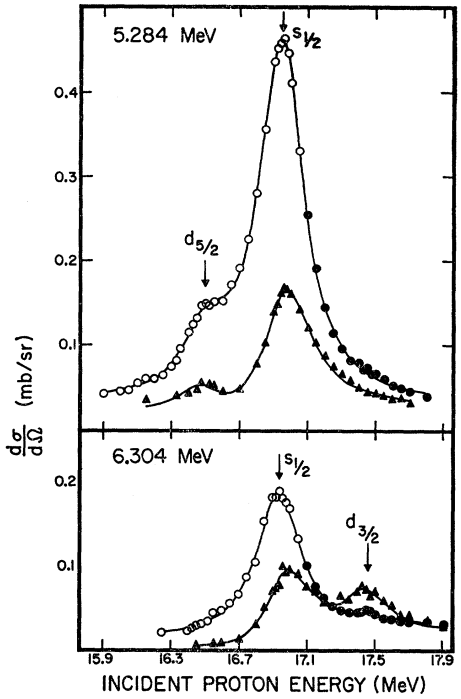

FIG. 8. ^{208}Pb$(p,p')^{208}$Pb excitation functions near the $s_{1/2}$ IAR. See also caption of Fig. 5.

5. $s_{1/2}$ (2.01-MeV) *Analog Resonance*

Only four states were strongly populated in the decay of the $s_{1/2}$ IAR. Because of resolution problems and small cross sections only two states could be adequately fit (see Fig. 8). The results are shown in Table V. The ratio of 90°/158° for the 5.284-MeV state is shown in Fig. 9. For an isolated resonance with no interference this ratio should be a constant with energy (for the $s_{1/2}$ resonance this constant should in fact be 1). The observed maximum between the $d_{5/2}$ and $s_{1/2}$ resonances can only be explained by either interference between the two levels or interference of both levels with the background or perhaps both effects. This ratio also yields a small effect near the $g_{7/2}$-$d_{3/2}$ resonances

TABLE V. Parameters for $s_{1/2}$ resonance.

^{208}Pb state E_{ex} (MeV)	θ_{lab}	E_0 (MeV)	Γ (keV)	σ_D (mb/sr)	σ_0/σ_D	N[a]
5.284	90°–100°	16.951	316	0.031	13.8	2
5.284	158°	16.981	322	0.021	6.9	2
6.304	90°–100°	16.953	322	0.015	11.3	2
6.304	158°	16.983	301	0.014	5.3	2

[a] See caption of Table I.

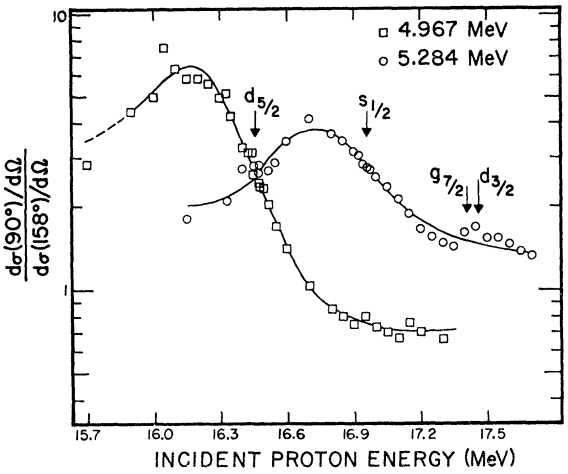

FIG. 9. Plot of ratio $[d\sigma/d\Omega(90°)]/[d\sigma/d\Omega(158°)]$ for the 4.967- and 5.284-MeV states in ^{208}Pb in the energy region of the $d_{5/2}$, $s_{1/2}$, $g_{7/2}$, and $d_{3/2}$ resonances. The solid line is the ratio of the fits shown in Figs. 7 and 8.

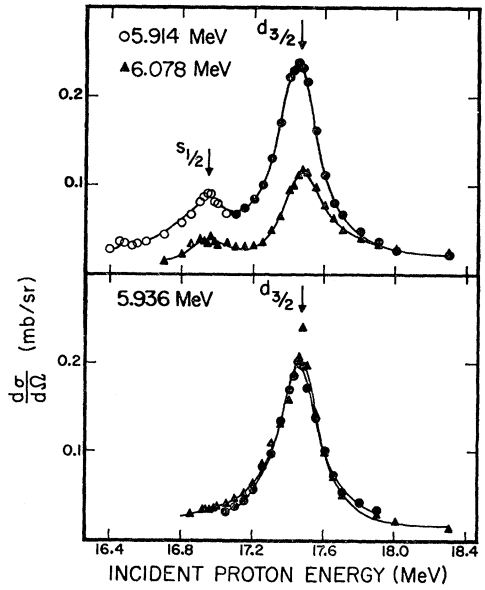

FIG. 11. ^{208}Pb$(p,p')^{208}$Pb excitation functions near the $d_{3/2}$ IAR. See also captions of Figs. 5 and 10.

although a resonance effect is less apparent for the excitation function at either angle.

6. $g_{7/2}$ (2.47-MeV)-$d_{3/2}$ (2.52-MeV) Analog Resonances

A total of 34 states between 5.769 and 7.200 MeV were observed to be populated by the decay of the $g_{7/2}$ and $d_{3/2}$ IAR. A resolution of 26 keV was not very adequate for separating these states. The experimental points for the 5.914- , 5.936- , and 5.958-MeV states shown in Figs. 10 and 11 have gone through a smoothing procedure. After the rough extraction of the excitation functions for two partly unresolved states is made, the

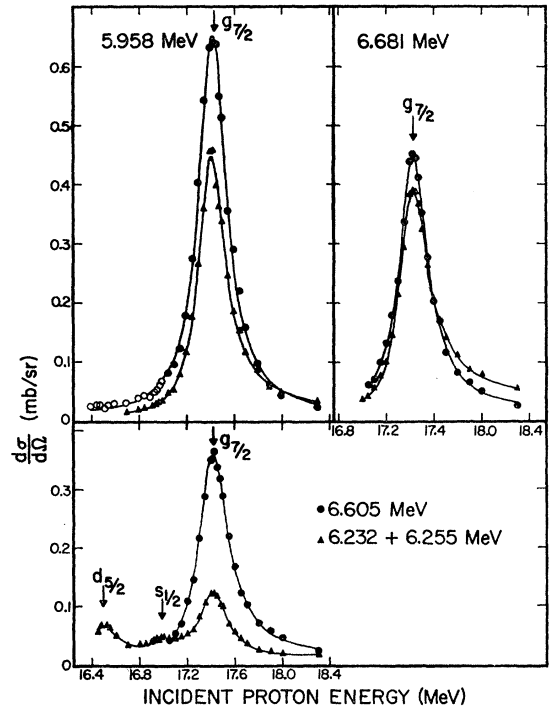

FIG. 10. ^{208}Pb$(p,p')^{208}$Pb excitation functions near the $g_{7/2}$ IAR. See also caption of Fig. 5. The open circles are data at $\theta_{lab}=90°$ normalized to match the data at $\theta_{lab}=100°$ (closed circles).

TABLE VI. Parameters for $g_{7/2}$-$d_{3/2}$ resonances.

^{208}Pb state E_{ex} (MeV)	θ_{lab}	E_0 (MeV)	Γ (keV)	σ_D (mb/sr)	σ_0/σ_D	N[a]
		Assignment $g_{7/2}$				
5.958	100°	17.438	283	0.011	60.2	1
5.958	158°	17.420	272	0.013	32.2	1
6.232 & 6.255	158°	17.435	267	0.009	12.1	3
6.377	100°	17.431	279	0.009	19.0	1
6.605	100°	17.427	298	0.011	11.5	1
6.681	100°	17.444	290	0.015	29.4	1
6.681	158°	17.426	297	0.028	12.7	1
5.869	90°–100°	17.417	280	0.020	14.0	3
5.869	90°–100°	17.416	276	0.006[b]		
5.869	158°	17.431	254	0.007	27.1	3
5.869	158°	17.419	251	0.001		
6.000	90°–100°	17.415	316	0.059	4.5	3
6.000	90°–100°	17.442	305	0.020[b]		
		Assignment $d_{3/2}$				
5.914	100°	17.471	277	0.017	13.0	2
5.936	100°	17.471	281	0.013	13.8	1
5.936	158°	17.491	275	0.014	13.6	1
6.078	158°	17.471	283	0.012	8.2	2
5.804	90°–100°	17.480	254	0.025	2.6	3
5.804	90°–100°	17.480	254	0.003[b]		
		No assignment				
6.409	158°	17.463	342	0.004	18.8	2[c]
6.540	158°	17.453	248	0.019	30.0	1
6.730	100°	17.443	308	0.013	29.9	1
6.730	158°	17.494	390	0.000	···	1
6.865	100°	17.457	298	0.005	26.4	1

[a] See caption of Table I.
[b] Value for σ_1 in mb/sr MeV. (See caption of Table IV.)
[c] The other resonance is the $s_{1/2}$.

cross section at a particular energy may be raised for one state and simultaneously lowered for the other so that the total cross section remains constant. In this manner, both excitation functions are simultaneously smoothed out. The smoothing procedure does not alter the characteristic shape of the original excitation functions. In addition to the resolution problems is the difficulty of determining which of the two analog resonances is populating the state of interest in ^{208}Pb. A total of 15 different states were fitted. On the basis of the value of the parameter E_0 we assigned either a $g_{7/2}$ or $d_{3/2}$ configuration to all but four of the states fitted (see Table VI). Undoubtedly some states assigned to one configuration also have a weak component of the other configuration, and subsequently the mixing of configurations causes errors in E_0 and Γ_{tot} for each resonance. The states not assigned a particular configuration probably have relatively equal contributions of $g_{7/2}$ and $d_{3/2}$ configurations. The fit for the 6.730-MeV state at 158° gave an unrealistically high value for Γ and a low value for σ_D.

7. *Discussion of Errors*

For the most part the errors in the parameters are those calculated by the fitting program and are the standard variances[15] for each parameter which is a measure of the goodness of fit for the given functional form. One estimate of the systematic errors was obtained by refitting the excitation functions with the energy-dependent background [Eq. (12)]. In the interest of space we do not present all these results, since we can summarize that for the cases studied (19 excitation functions), the resonance energy showed an average magnitude shift of 8 keV with a random sign. The shift was usually in the direction of lowering the root-mean-square deviation of all the energies and widths. A shift upward in energy was usually accompanied with a decrease in the value of Γ and vice versa. The average shift in Γ was about 7 keV.

Another indication of the error in determining Γ is obtained by noting that the full width at half-maximum W of the cross section $\sigma(\theta,E)-\sigma_D$ is closely related to

$$W\approx\Gamma[1+\tfrac{1}{4}(S/\sigma_0)^2]+O(S/\sigma_0)^4 \qquad (13)$$

for the case of one resonance and an energy-independent background. The formula shows that W and Γ are nearly the same since $(S/\sigma_0)^2<0.1$ for nearly all cases studied. The Γ extracted from the data depends critically on the proper value of $\frac{1}{2}\sigma_0$ which further depends on knowing σ_D accurately. This emphasizes the advantage of fitting the resonances with Eq. (8).

The statistical errors can be deduced from the experimental curve using the following conversion factors 0.1 mb/sr≈1000 counts for the 90° data and 0.1 mb/sr≈1600 counts for the 158° data.

B. Refit of the Elastic Scattering

Partial proton widths were obtained from an analysis of the elastic-scattering data of Zaidi *et al.*[3] using the formalism outlined in their paper. Fits to the data were obtained using a nonlinear least-squares fitting program ELSCAT, written for the SDS 930 on-line computer, which allowed up to 33 parameters (five background and four for each of seven resonances) to be varied simultaneously. The program allows selected parameters to be held fixed while the others are varied. The data points were not weighted and errors in final values of the varied parameters were computed in the usual way.[15]

The 170° elastic-scattering cross section has a more pronounced structure than those at 90°, 125°, and 150°, but it was not possible to vary all parameters (three background and four by six resonance parameters) at once, the difficulty being caused by the closely spaced $g_{7/2}$ and $d_{3/2}$ resonances. A number of sets of parameters were found that gave equally good fits to the data. Some of these sets gave parameters that differed by almost a factor of 2 from corresponding ones in other sets. For example, good fits were obtained when the $g_{7/2}$ proton width was 48 or 26 keV. Also some sets gave values for the total widths, and resonance energies well outside the limits found from the analysis of the inelastic-scattering data. Because of these difficulties, total widths and resonance energies were held fixed at the values obtained from the inelastic scattering measurements (see Table VIII). All resonance energies were increased by 20 keV from the data in Ref. 3 to account for slightly different energy calibrations. With this restriction it was found that if the fitting procedure converged it always gave the same final set of parameters for different initial parameters. The results of the 170° analysis is given in Table VII.

The 150° elastic-scattering data were fitted using the values E_0 and Γ determined in the present experiment. At this angle the g-wave resonances show nearly no effect as the interference term is near a zero of P_4. It

TABLE VII. Elastic-scattering parameters. All fits were obtained with the values of Γ and E_0 held fixed at the best-fit values for the inelastic scattering given in Table VIII. The errors quoted are fitting errors only and do not represent the total errors of the measurement of these quantities.

	Γ_p (keV)					α_{lj} (rad)[a]
	170°	150°	125°	90°	Ref. 3	170°
$g_{9/2}$	19.6±0.2	···	18±1	20.6±1.0	22±3	2.54
$i_{11/2}$	2 ±0.3	2.0±4	1±1	3 ±1	···	−0.88
$d_{5/2}$	44 ±1	51 ±3	···	38 ±2	30±3	0.93
$s_{1/2}$	42 ±2	48 ±6	55	46 ±4	175±10	−0.17
$g_{7/2}$	43 ±4	···	50	60 ±14	30±6	3.38
$d_{3/2}$	35 ±7	28 ±2.5	···	50 ±19	40±8	−5.38

[a] α is the phase as defined in Ref. 3.

[15] A. J. Ferguson, in *Angular Correlation Methods in Gamma Ray Spectroscopy* (Interscience Publishers, Inc., New York, 1965), Chap. 4.

was found that by varying the fit to the background (off-resonance) cross section, different proton partial widths could be found which gave equally good fits to the resonances. All values were within the fitting errors except for the $s_{1/2}$ resonance for which values between 44 and 53 keV were obtained. The error for the $s_{1/2}$ resonance partial width is thus approximately ± 6 keV for this angle.

The 125° data yielded very little new information for the following reason: The $d_{5/2}$ and $d_{3/2}$ resonances should show a small effect according to the formalism of a single resonance plus interfering background; however, the observed effect was larger than could be predicted. It was therefore only possible to obtain fits to the $g_{9/2}$ resonance. We were able to reproduce the cross section for all the resonances fairly well by using the values of Γ_p given in Table VII and by adding, empirically, an equal contribution from the $d_{5/2}$ and $d_{3/2}$ resonances. It is difficult to calculate the errors in this approach but they are estimated at 20% for the $s_{1/2}$ and $g_{7/2}$ partial widths.

Fits to the 90° cross section could be obtained using three, four, or five background parameters,[3] which had the effect of giving widely different values of Γ_p for the $g_{7/2}$ and $d_{3/2}$ partial widths. The values and errors quoted in Table VII for the 90° data are those calculated for the case of five background parameters. The fitting errors are seen to be large for the $g_{7/2}$ and $d_{3/2}$ resonances and are thought to be not too conservative because the fits using only three-background parameters gave partial widths barely within the range of these errors.

In summary, even with predetermined values of the total widths and resonances energies, it is seen that there is still some difficulty in obtaining consistent elastic partial widths at various scattering angles in the case where the resonances are overlapping. The fit with the smallest errors and the apparently more stable fit is for the 170° data that have the largest resonance effect and the smallest effect from background cross sections. The partial widths for the $g_{9/2}$, $i_{11/2}$, and $s_{1/2}$ resonances are very consistent at the different angles, and the $g_{7/2}$ is slightly less consistent. The $d_{5/2}$ and $d_{3/2}$ values are found to be rather inconsistent for the three-angles fit, and this inconsistency does not manifest itself in the fitting errors at a given angle.

Note that the fitting formula assumes that the direct spin-dependent scattering amplitude can be neglected. While this is a very good assumption for the angle $\theta=170°$, it may be less good for the other angles. It seems impossible, however, to take this effect into account without much better experimental data.

V. CONCLUSIONS

By doing careful excitation functions and using a consistent analysis procedure as discussed in Sec. III, we were able to obtain a consistent set of resonance parameters for each IAR. This consistency is an important check on the validity of the collision matrix consisting of a constant background amplitude and a Breit-Wigner term for the analysis of inelastic-scattering cross sections for analog states and it allows us to identify the fit parameters E_0 and Γ with the resonance energy and the total widths of the analog resonance in question.

The results of each resonance which are summarized in Tables I–VI leads to the final parameter values given in Table VIII. The errors quoted are fitting errors calculated by the program plus contributions estimated from the analysis using Eq. (12) (see Sec. IV A 7).

In Table VIII we also give the excitation energies calculated for the parent analog states together with those obtained from ^{208}Pb(d,p).[16] The agreement in energies is striking.

Using our $g_{9/2}$ resonance energy, we obtain a Coulomb displacement energy of $\Delta E_c = E_p{}^{\text{c.m.}} + S_n = 14.847 \pm 0.006 + 3.943 \pm 0.011$ MeV $= 18.790 \pm 0.013$ MeV.

TABLE VIII. ^{209}Bi* single-neutron analog resonance parameters.

	$E_{\text{res}}{}^{\text{lab}}$ (MeV)	Γ (keV)	$E_{\text{res}}{}^{j} - E_{\text{res}}{}^{g_{9/2}}$[a]	$E_{\text{ex}}(^{209}\text{Pb})$[b]
$g_{9/2}$	14.918±0.006	253±10	0	0
$i_{11/2}$	15.716±0.010	224±20	0.794	0.79
$j_{15/2}$	16.336±0.015	201±25	1.411	1.42
$d_{5/2}$	16.496±0.008	308±8	1.570	1.56
$s_{1/2}$	16.965±0.014	319±15	2.037	2.01
$g_{7/2}$	17.430±0.010	288±20	2.500	2.47
$d_{3/2}$	17.476±0.010	279±20	2.545	2.51

[a] These are c.m. energies.
[b] Energies of ^{208}Pb states are taken from Ref. 16.

In addition to the resonance parameters the particles J forming the neutron particle contribution to the neutron particle-hole configurations of the ^{208}Pb states are determined for most of the states studied. The background reaction cross sections are also determined for 90° and 158°.

Using the best-fit parameters for E_0 and Γ, the elastic-scattering data[3] were refitted and reasonably consistent values of Γ_p were obtained. Closely lying levels remain difficult to analyze in the elastic channel since the resonance phase was used as a free parameter.

ACKNOWLEDGMENTS

The authors wish to thank Professor C. F. Moore and H. Wieman for assistance in taking data and Dr. J. Bondorf for interesting discussions.

[16] G. Muehllehner, A. S. Poltorak, W. C. Parkinson, and R. H. Bassel, Phys. Rev. **159**, 1039 (1967).